J. Condensed Matter Nucl. Sci. 38 (2024) 1–12

Research Article

Reproduction of Excess Heat of Pd-B Cathode Measured by Seebeck Calorimeter

Wu-Shou Zhang*

Institute of Chemistry, Chinese Academy of Sciences, Beijing 100190, China

Abstract

Clear excess power from a Pd-B rod cathode provided by Melvin H. Miles was measured with a Seebeck calorimeter during D_2O electrolysis. A reflux open-electrolytic cell, with the advantage of small constant power of D_2O evaporation in electrolysis ($P_{vapor} = 0.00979I$ at 25°C, the working temperature of calorimeter) was used and the calorimetry was therefore simplified. It was verified that pre-electrolysis of the cathode in open cell under high current and high temperature is an effective activation method for excess heat production in subsequent electrolysis. However, only the second activation gave the maximum excess power of 0.15 W with input power of 3 W and more activation was useless. After checking past results on excess heat of Pd plate samples in our lab, it is also found that the activation of cathode must be limited to a couple of times. On the other hand, after a long duration of intermittent electrolysis, the volume of the Pd-B electrode increased very little, meeting the requirement of volume expansion of excess-heat-producing Pd samples discovered by Edmund Storms.
 ISSN 2227-3123

Keywords: Excess heat, Heavy water, Pd-B rod, Reflux open-electrolytic cell, Activation, Excess volume.

1. Introduction

It is well known that excess heat occurring in Pd/D_2O systems was first found in open-electrolytic cells by using isoperibolic calorimetry (IPC) by Fleischmann and Pons [1], [2] and reproduced afterwards in closed-electrolytic cells with mass flow calorimetry (MFC, e.g., the method used by McKubre et al. [3]) and Seebeck envelope calorimetry (SEC, e.g., Storms [4]). Since then, Melvin H. Miles and his co-workers have been studying excess heat in open Pd/D_2O electrolytic cells with IPC, in detail, for more than 30 years [5]–[8]. Miles and Imam reported that Pd-B rod can give reproduceable excess heat [7]. During the satellite meeting of ICCF20 in 2016, Xing Zhong Li suggested me to measure excess heat with samples of Miles using our SEC, which had been shown to detect significant excess heat in closed Pd/D_2O electrolytic systems [9]–[11]. In May 2017, Miles delivered one Pd-0.25wt.%B rod and other 3 samples to me. The rod is 4.71 mm in diameter and 20.1 mm in length, volume of 350.2 mm^3, area of 3.3227 cm^2 and weight of 4.1177 g (measured with an Ohaus PX224ZH balance) as shown in the left of Fig. 1. This batch was made at

*Corresponding author: wszhang@iccas.ac.cn or zhangwushou@hotmail.com

 ISSN 2227-3123

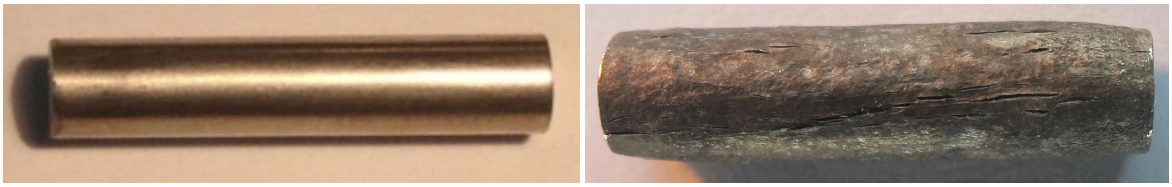

Figure 1. Pd-0.25wt.%B rod from M. H. Miles. (left) new sample; (right) the sample after electrolysis for 2,147 h (89.5 d).

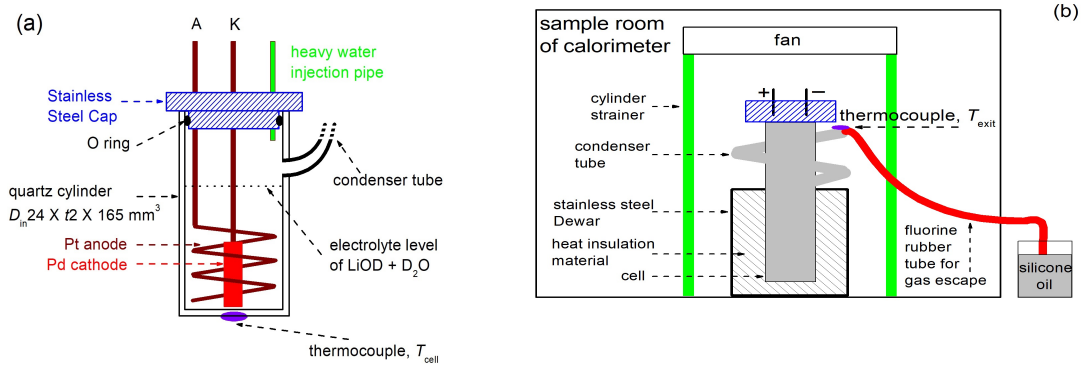

Figure 2. Schematics of Pd/D_2O reflux open-electrolytic cell (a) and the cell with calorimetric attachments (b). All components shown here are placed in a Seebeck calorimeter, as described in previous literatures [9]–[12].

NRL by M. Ashraf Imam, which had produced the maximum excess power of 0.24 W [7]. This sample became stumpy (4.62 $\sim$ 4.94 in diameter and 19.1 mm in length) with weight of 4.1156 g after a long duration of electrolysis as shown in the right of Fig. 1. At ICCF-23, the primary results of excess heat produced by this sample was reported [12]. This paper presents all results.

2. Experimental Set-Up and Calorimetry of Reflux Open-Electrolysis

2.1. Experimental Set-Up

We designed a reflux open-electrolytic cell as shown schematically in Fig. 2(a). The electrolytic cell is a quartz tube (ϕ_{in}24 mm, ϕ_{out}28 mm and h165 mm) with a curved branch tube and a stainless-steel lid. The branch tube is in a spiral shape (1 cm in tube diameter, 7 cm in spiral diameter, around 3 circles or 65 cm long). The branch tube serves as the outlet for the evolving gas and vapor, and as the condenser tube. It enters the cell at a position 9.4 cm high, which is above the waterline, as shown in Figs. 2 and 3. The anode is a spiral Pt wire (ϕ0.5 mm and l1.4 m, 99.95%, GRINM, Beijing). The electrode leads are Pt wires (ϕ1.1 mm and l18 cm each, 99.99%, GRIKIN, Beijing) covered with PTFE heat shrinkable tubes to prevent catalyzing $D_2 + O_2$ recombination. D_2O (99.8at.%) is from J&K Chemical. Li_2O powder (99.5%, Alfa Aesar) is dissolved in heavy water to make a 0.1 M LiOD solution. An injection pipe made of stainless-steel is fixed in the lid for periodic heavy water addition. Four different O-rings (not all shown in Fig. 2(a)) are used around the lid, the two leads and the injection pipe to prevent gas from escaping through the lid. A K-type thermocouple is attached to the bottom of the cell to measure temperature (T_{cell}). The top part of the cell, the lid with two leads and electrodes, is not taken part after each run. Li_2SiO_3 sediment sometimes appears on the inner wall of the

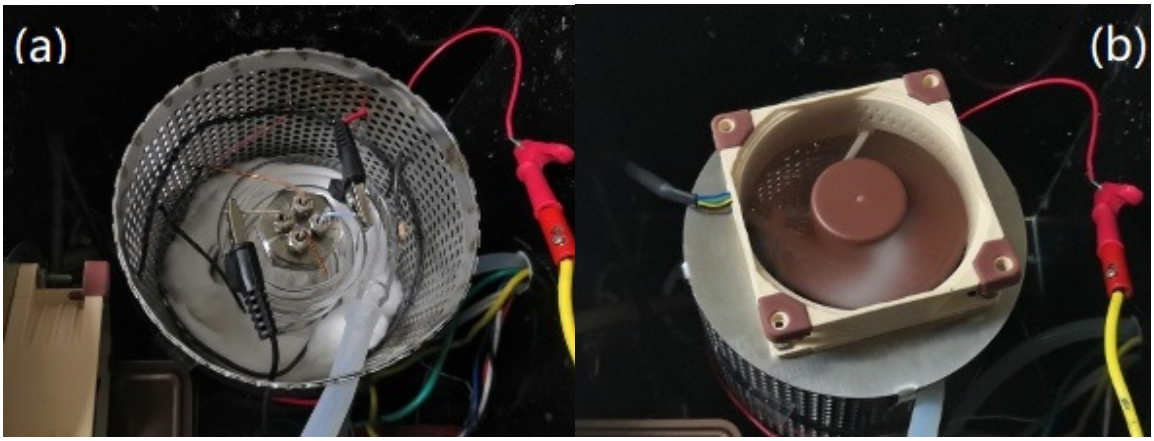

Figure 3. Photos of electrolytic cell with heat insulation (a) and fan (b) in the Seebeck calorimeter.

cell and the surfaces of two electrodes, when temperature is higher than 80°C, especially in activation experiments [12]. Then this happens, the whole cell has to be taken part and cleaned in water and ethanol, and dried in an electric constant temperature blast drying oven (80°C for 1 h).

The electrolytic cell is placed in the center of a stainless-steel Dewar (ϕ_{in}75 mm, ϕ_{out}83 mm, h_{in}103 mm and h_{out}120 mm) with cotton wool between the gap as heat insulation material to increase the cell temperature, as shown in Figs. 2(b) and 3(a). The Dewar is placed in the center of a cylinder strainer (ϕ12 cm and h23 cm), which is covered with a fan blowing the air downward to ensure even temperature distribution in the sample chamber of the SEC, as shown in Figs. 2(b) and 3. To make the heavy water vapor further condense, a fluorine rubber tube (ϕ_{in}10 mm, ϕ_{out}14 mm and l2 m) is connected to the condenser tube of the cell at one end, and another end is immersed in the silicone oil outside of the SEC to prevent contamination from air, as shown in Figs. 2(b) and 3(a). A K-type thermocouple is attached to the end of the condenser tube to monitor the temperature of the exit (T_{exit}), as shown in Figs. 2(b) and 3(a). Gases produced in electrolysis, including oxygen, deuterium and heavy water vapor, all escape through the tubes. It should be noted that T_{cell} and T_{exit} are only used for reference in the electrolysis process. The output power of the electrolytic cell (P_{SEC}) is measured by 18,796 thermocouples in a Seebeck calorimeter as reported previously [10].

To replenish heavy water consumed by electrolysis and evaporation, a syringe pump with injector was used to add heavy water into the electrolytic cell through the injection pipe shown in Fig. 2(a). It was used in the long duration electrolysis experiments, Exp. #201127 to 210322, as summarized in Table 7 in the previous work [12]. The syringe injection pump was not used after that. The purpose of this work was to find a way to activate the Pd sample, rather than continuously monitor for excess heat for a long duration, as was done in early cold fusion research. With our method, the electrolysis time was generally controlled within 48 h (except in Exp. #220222 in which it lasted 60 h).

2.2. Calorimetry of Reflux Open-Electrolysis

The excess power P_{ex} in the D_2O reflux open-electrolytic cell shown in Figs. 2 and 3 under steady state (input power is constant, i.e., $dP_{in}/dt = 0$) can be expressed as [12]

$$P_{ex} = P_{SEC} + P_{vapor} - (V_{cell} - V_{th})I \quad (1)$$

where P_{SEC} is the thermal power measured by SEC; V_{cell} is the cell voltage; $V_{\mathrm{th}} = 1.52666$ V at 25°C (the working temperature of SEC), the thermoneutral potential of heavy water ($V_{\mathrm{th}} = 1.48121$ V for light water at 25°C); I is the electrolysis current; P_{vapor} is the evaporation power and it can be expressed as

$$P_{\mathrm{vapor}} = 0.75 \frac{I}{F} \frac{p}{p* - p} L_{\mathrm{D_2O}} \tag{2a}$$

$$= 0.00979 I \ @ \ 25^{\circ}\mathrm{C} \tag{2b}$$

where F is the Faraday constant; $p^* = 1.01325$ bar, the atmosphere pressure; $L_{\mathrm{D_2O}} = 45.402$ kJ/mol, the evaporation enthalpy of heavy water at 25°C; $p = 0.02735$ bar, the evaporation pressure of heavy water at 25°C. Because p is a small value at room temperature, therefore P_{vapor} does not change prominently with p^* as in the Fleischmann-Pons-Miles situation [2], [5]–[8]. For light water, the coefficient in Eq. (2b) is 0.01104 at 25°C.

Our experimental results also indicate that only the D_2O evaporation at ambient temperature, and not the cell temperature, needs to be considered for reflux open-electrolysis. The maximum temperature increment ΔT_{exit} of the condenser-tube end (see Figs. 2(b) and 3(a)) during electrolysis was 2.6°C when the cell temperature (T_{cell}) was 96°C in Exp. #200713 (where D_2O vapor pressure is 0.83 bar at this temperature). This also verifies that the vapor is cooled to around the ambient temperature through the condenser tube. Because there is another 50 cm of rubber tube to condense the D_2O in the sample chamber of the SEC, there is no doubt about the validity of Eqs. (1) and (2). The validation of Eq. (2) is also verified by the mass change during electrolysis. As shown in the previous work [12], at 25°C, the evaporation of D_2O will induce 4.16% more mass loss than that of electrolysis alone. In most cases, the difference between the theoretical and actual mass losses in our experiments was less than 1%. For example, in Exp. #210327, electrolysis currents and times of 0.7 A × 36 h, 0.6 A × 4 h and 0.5 A × 8 h were applied successively, and a total of 9.6 ml of heavy water was added 3 times during electrolysis. The theoretical mass-loss according to this model is 12.3372 g, the actual loss was 12.3184 g, so the difference is only 0.0188 g or 0.15%.

In other words, the reflux open-electrolytic cell is an effective design to reduce the evaporation process' influence on power balance, which was the biggest uncertainty omitted or debated in the calorimetry of open electrolysis in past works [2], [5]–[8].

Because the open-electrolyzing process is usually unsteady ($\mathrm{d}P_{\mathrm{in}}/\mathrm{d}t \neq 0$), we need to use the combination of the average excess power $\overline{P}_{\mathrm{ex}}$ ($= Q_{\mathrm{ex}}/t$, the total excess heat divided by the electrolysis time) and P_{ex} of Eq. (1) to determine whether there is excess heat or not. Another approximation is to consider the change of input power over time, $\mathrm{d}P_{\mathrm{in}}/\mathrm{d}t$, the modification of excess power in Eq. (1) is approximated in the first order:

$$P'_{\mathrm{ex}} \ = \ P_{\mathrm{ex}} \ + \ C \frac{\mathrm{d}P_{\mathrm{in}}}{\mathrm{d}t} \tag{3}$$

where C is the correction coefficient, which depends on the thermal properties of the whole system (e.g. the open cell and materials around it, and the calorimeter). P'_{ex} is closer to $\overline{P}_{\mathrm{ex}}$ than P_{ex} is. However, Eq. (3) is only applied in data analysis after the data-logging is completed while the input power changes slowly and linearly with time.

In our experiments, the cell voltage and current, temperatures and calorimetric signals are all recorded on a computer, in real-time, every second.

3. Results

3.1. Calibration and Trial Results

In the last 7 years, a new technique which can eliminate most thermal noise caused by temperature fluctuation of the circulating bath of the SEC was developed in our lab [12], [13]. An example of the calibration in Exp. #210315 using this technique is shown in Fig. 4, the standard deviation is only 1.3 mW this time and is one order smaller than

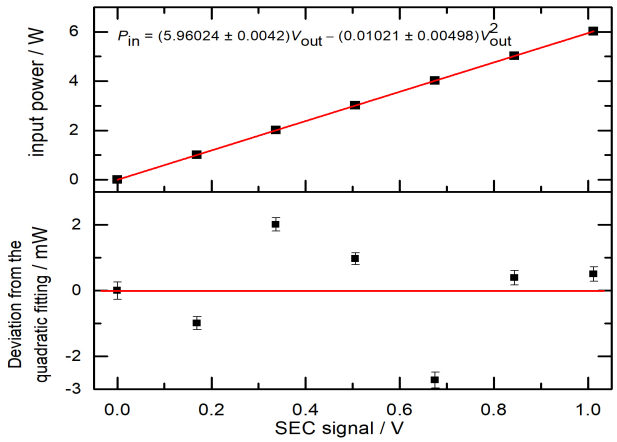

Figure 4. Calibration result of the SEC with an electric heater at 25°C in Exp. #210315.

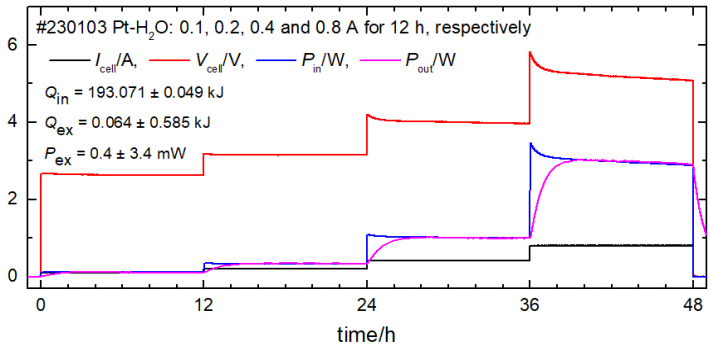

Figure 5. Zero excess heat in Exp. #230103 for Pt-H_2O reflux open-electrolysis.

before [9]–[11]. This technique ensures that the sensitivity and accuracy of the decimeter-sized sample chamber of the SEC can approach the levels of IPC of Fleischmann-Pons-Miles [2], [5]–[8].

The calorimeter was calibrated with a resistor in the electrolytic cell every month to ensure the accuracy of calorimetry. They gave the same results in the measurement error of milliwatts.

Before the report of excess heat production, some trivial results are introduced. Fig. 5 shows an example of calorimetry on Pt-H_2O system in Exp. #230103, where a Pt wire cathode (ϕ0.5 mm and l14.6 cm), a Pt plate anode (0.05 mm $\times$ 2 cm^2) and 0.1 M H_2SO_4 solution was used. The cathode and anode in previous experiments were exchanged in this run; therefore, the cathode showed no excess heat production because of no deposition [12]. The electrolytic current was stepped through 0.1, 0.2, 0.4 and 0.8 A successively, with each step applied for 12 hours. It is shown that total excess heat is 0.064 kJ, which is only 11% of the standard deviation. At 0.8 A, the instantaneous excess power $P_{ex} = 32 \pm 5$ mW, which is just a non-equilibrium effect due to $dP_{in}/dt = -16$ mW/h. Because $P'_{ex} = 0$, the correction coefficient C in Eq. (3) is 2 h/mW. In Exp. #201227 for a Pd-D_2O open-electrolytic cell, $C = -2.93$ h/mW, as shown in Fig. 15 of Ref. [12]. These two values of C are of a similar order of magnitude.

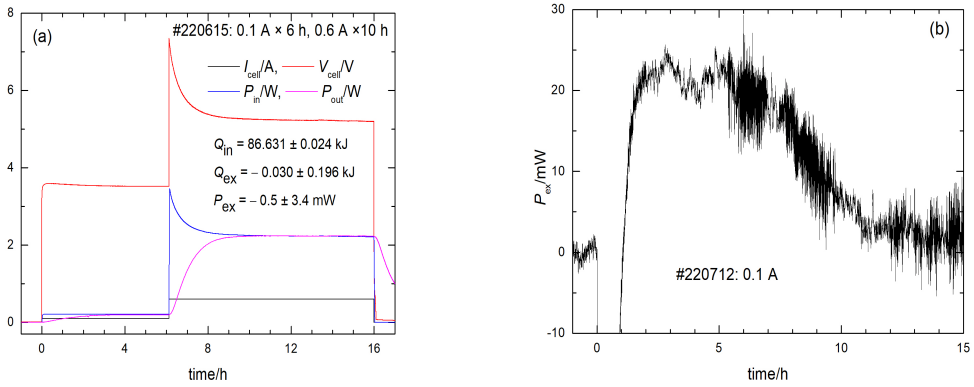

Figure 6. (a) zero excess heat in Exp. #220615; (b) formation heat of palladium deuteride in Exp. #220712.

Table 1. Effects of activation on excess power production of Pd-B rod.

#	$T_{\mathrm{activ,max}}$/°C	R	$\overline{P}_{\mathrm{ex,max}}$/mW	I/A	t/h	date range
0		1/7	21(7)	0.5-0.75	387	201223-210129
1	218	2/11	46(3)	0.17-0.7	436	210202-220206
2	94	11/12	130(2)	0.1-1.2	371	220220-220330
3	97	1/4	22(7)	0.1-0.6	86	220401-220419
4	96	6/13	43(7)	0.05-0.6	629	220421-220623
5	96	3/6	42(3)	0.1-0.7	130	220626-220709
6	96	0/2	6(2)	0.1-0.7	54	220711-220714

Note: # is the ordinal number of cathode activation, which is putting the cathode in an open cell and electrolyzing under high current (< 4 A) and high temperature for less than 11 h. The electrolyte is D_2SO_4 in #1 and LiOD heavy water solution in #2 to 6; $T_{\mathrm{activ,max}}$ is the maximum temperature of cell reached during activation; R, $\overline{P}_{\mathrm{ex,max}}$, I and t are the reproducibility, the maximum average excess power, the current applied and the total electrolysis time, respectively, in the subsequent runs of electrolysis and calorimetry.

Two other examples of zero excess heat are shown in Fig. 6, for Pd-B/D_2O electrolysis while the cathode is inactive. In the first example (Fig. 6(a)), 0.1 A was applied for 6 h and then 0.6 A was applied for 10 h in Exp. #220615. The total excess heat is -0.030 $\pm$ 0.196 kJ with the total input heat of 86.631 $\pm$ 0.024 kJ. The average excess power is -0.5 ± 3.4 mW, which is equivalent to zero within the standard deviation. At 0.6 A, the instantaneous excess power $P_{\mathrm{ex}} = 15 \pm 4$ mW and $\mathrm{d}P_{\mathrm{in}}/\mathrm{d}t = -5$ mW/h; therefore $C = 3$ h/mW as done before.

Fig. 6(b) shows another example of calorimetry from Exp. #220712, where the Pd-B cathode was heated to 80°C in an electric constant temperature blast drying oven for 1 h before calorimetry was performed, and the absorbed deuterium in previous runs was desorbed. The average excess power is 21 $\pm$ 2 mW in the first 7 h, the total excess heat is 0.602 $\pm$ 0.172 kJ, while the formation heat of palladium deuteride is 0.593 kJ (calculated as $PdD_{0.6}$ stoichiometric number). This means the excess heat in the first 10 h is only from the formation heat of palladium deuteride.

3.2. Excess Heat With Pd-B

A total of 6 runs with activation and 55 runs of calorimetry were tested for the Pd-B rod from Dec. 2020 to July 2022 as listed in Table 1. The cumulative electrolysis duration was 2,147 h (including 54 h of activation). The appearance of Pd-B rod in the fresh as-received condition, and after electrolysis, are shown in Figs. 1(a) and (b), respectively.

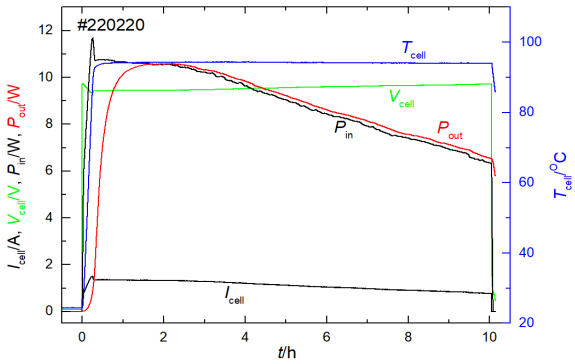

Figure 7. Electrolytic parameters in the second activation in Exp. #220220.

It is found that the Pd-B rod changed from brightness and uniform to darkness, rough and uneven due to repeated deuteriding-dedeuteriding.

In the first 7 runs of Exp. #201223 to 210129 (see also Table 7 in Ref. [12]), the Pd-B cathode was used as received and only cleaned with ethanol before the first run. However, it only produced maximum average excess power of 21 $\pm$ 7 mW in Exp. #201225 as listed in Table 1 and reported previously [12]. After that, the Pd-B cathode was treated with the activation method described before [9], [11]. Firstly, the cathode was open-electrolyzed in concentrated D_2SO_4 heavy water solution in another cell for 3.6 h on Feb. 2, 2021; the DC power was set at 4 A and 18 V; the maximum temperature of cell reached 218°C. Then the cathode was cooled naturally and cleaned. Finally, the cathode was assembled in the reflux open-cell and it was electrolyzed and conducted calorimetry. It showed more excess power than the previous series, the maximum average excess power of 46 $\pm$ 3 mW occurred in Exp. #210306 in all 11 runs (Exp. #210202 to 220206). However, the reproducibility was only 2 out of 11 tests as listed in Table 1.

On February 20, 2022, we tried a second activation run, as shown in Fig. 7. At this time, the electrolyte of 0.1 M LiOD heavy water solution and the reflux open-electrolytic cell were used; the DC power was set as 2 A and 10 V; the electrolysis duration was 10 h; the actual current decreased from 1.5 A at the beginning to 0.76 A at the end; the maximum temperature of the cell reached 94°C.

In subsequent electrolysis of Exp. #220222, average excess power of 70 $\pm$ 2 mW with average input power of 3.2 W was observed. In Exp. #220226, average excess power of 53 $\pm$ 2 mW at 0.1 A were observed ($\overline{P}_{ex}/\overline{P}_{in} = 18\%$, see Fig. 8(a)). In Exp. #220228, average excess power of 130 $\pm$ 2 mW at 0.6 A were observed ($\overline{P}_{ex}/\overline{P}_{in} = 5\%$); the total excess heat in this run was 22.488 $\pm$ 0.332 kJ as shown in Fig. 8(b).

The comparison of two experiments with and without excess power is shown in Fig. 9. In Exp. #210318 shown in Fig. 9(a), no excess power was observed while 0.7 A was applied for 36 h after first activation. In Exp. #220228 shown in Fig. 9(b), instantaneous excess power reached 0.2 W after the second activation. Another interesting point is that the temperature of cell was 82°C in both runs; however, the input power was 3.6 and 3 W in Exp. #210318 and #220328, respectively. This also indicates the excess power was produced in the latter run. Even if the linear correction of the input power is taken into account as in Eq. (3) and $C = 3$ h/mW as obtained in Section 3.1, $P'_{ex} = -4 \pm 13$ mW for the case shown in Fig. 9(a) with $dP_{in}/dt = 1.3$ mW/h (see Table 7 in Ref. [12]), and $P'_{ex} = 168 \pm 26$ mW for the case shown in Fig. 9(b) with $dP_{in}/dt = -8.5$ mW/h (see Table 2). The conclusion remains that the experiment shown in Fig. 9(b) produces significant excess power.

Excess heat results of open-electrolytic system with the Pd-B rod after the second activation, as shown in Fig. 7, are summarized in Table 2. Nearly all of runs gave excess power at different currents and different temperature, except for

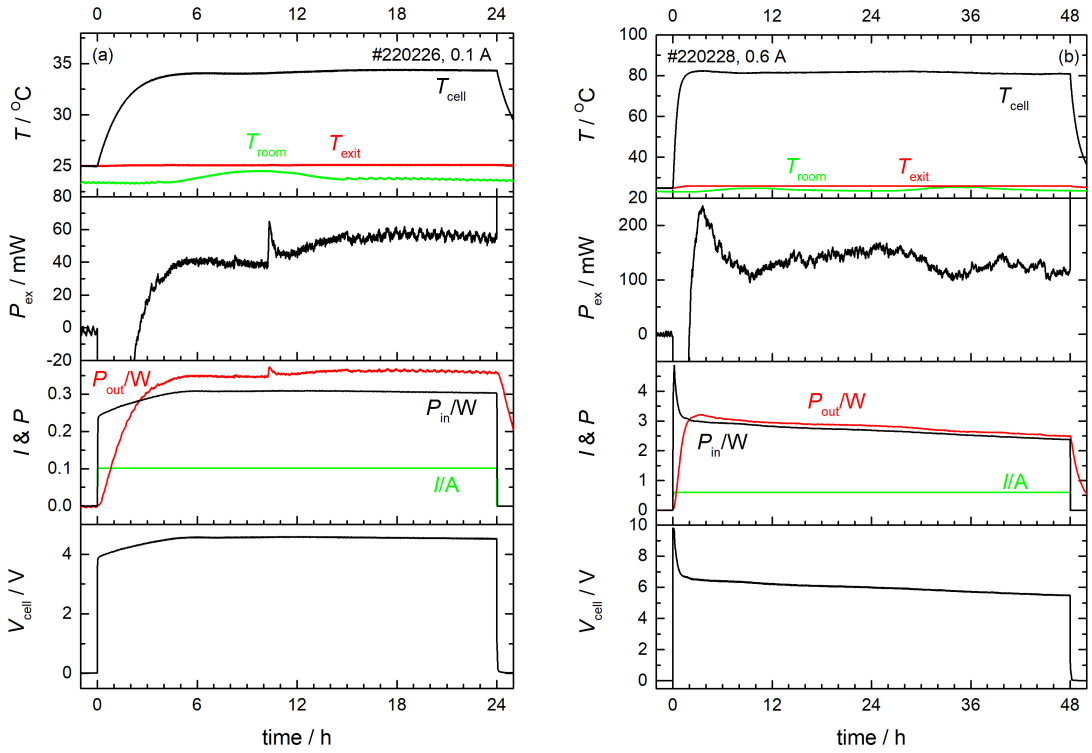

Figure 8. Electrochemical and calorimetric parameters of Pd-B/D_2O system in Exp. #220226 (a) and #220228 (b).

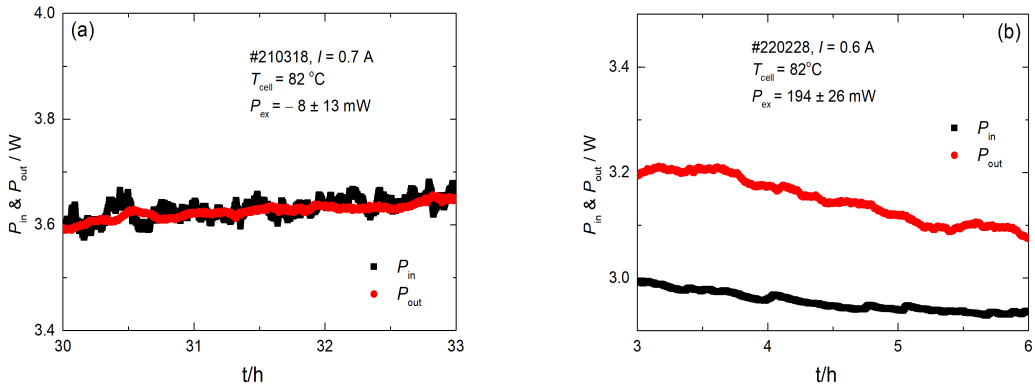

Figure 9. (a) Input and output power of Exp. #210318, no excess heat was produced, and the Pd-B cathode was inactive at that time; (b) Input and output power of Exp. #220228, sustained excess heat was produced, indicating that Pd-B cathode was active.

Table 2. Summary of excess heat in Pd-B/D_2O+LiOD reflux open-electrolytic cell after second activation.

	Integrated values				Steady values				
Exp. #	$I \times t$	Q_{in}	Q_{ex}	$\overline{P}_{ex}$	period	P_{in}	P_{ex}	dP_{in}/dt	T_{cell}
	A × h	kJ	kJ	mW	h	W	mW	mW/h	°C
220222	0.1 × 18, 0.6 × 30, 1.2 × 11, 0.6 × 13	838.61(15)	18.23(52)	70(20)	6 - 8	0.254(1)	32(1)	0.35	31
					28 - 32	2.730(16)	158(8)	−16	76
					50 - 53	9.504(16)	122(14)	−18	92
					62 - 64	3.612(3)	52(14)	36	88
220226	0.1 × 24	26.047(2)	4.62(17)	53(2)	22 - 24	0.304(0)	55(2)	−0.55	34
220228	0.6 × 48	466.67(9)	22.49(33)	130(2)	20 - 24	2.710(11)	149(6)	−8.5	82
220303	0.6 × 11		NA		4 - 6	2.986(22)	39(18)	−15	78
220304	0.6 × 48	484.61(9)	3.98(33)	23(2)	12 - 16	2.781(24)	85(16)	6.1	77
220317	0.6 × 24	272.48(5)	5.06(54)	59(6)	20 - 24	3.126(5)	53(3)	−3.6	26
220319	0.6 × 24	226.47(5)	3.34(63)	39(7)	9 - 12	2.603(4)	44(3)	−4	73
220322	0.6 × 24	241.92(5)	1.43(63)	17(7)	11 - 13	2.786(4)	6(7)	3.6	82
220324	0.6 × 24	278.01(5)	4.00(56)	46(6)	4 - 7	3.151(8)	40(3)	17	46
					22 - 24	3.305(1)	55(4)	0.56	NA
220326	0.6 × 24	329.92(6)	4.24(58)	49(7)	9 - 10	3.601(18)	−10(4)	66	41
					23 - 24	4.734(20)	-5(6)	86	47
220328	0.6 × 24	227.20(4)	3.87(50)	45(6)	22 - 24	2.511(6)	42(4)	−11	42
220330	0.6 × 24	166.44(4)	1.89(64)	22(7)	9 - 11	1.847(7)	42(5)	−12	71

Note: Q_{in} is the total input energy; Q_{ex} is the total excess heat; $\overline{P}_{ex} = Q_{ex}/t$, the average excess power.

Exp. #220303 due to a calorimetric problem. Of course, high current or high temperature will give more excess power than low current and low temperature. One example is shown in Exp. #220222 as listed in Table 2. It was found that $P_{ex} = 32$ mW at 0.1 A (31°C) and $P_{ex} = 158$ mW at 0.6 A (76°C). However, $P_{ex} = 122$ mW at 1.2 A (92°C), which is less than that at 0.6 A because the input power was overestimated due to bubble formation and unstable voltage recording, as discussed in Ref. [12]. In any case, the excess power depends mainly on the activity of the sample itself. The first several runs gave the most prominent excess power. After then, excess power decreased with time in a random manner.

After the first two activations and subsequent runs of electrolysis and calorimetry, this process was repeated 4 times from April to July 2022 as listed in Table 1. However, the excess heat was not as prominent as the second series.

4. Discussions

In previous works [9], [11], we found that 3 activation methods of (1) pre-electrolysis under high current and temperature, (2) heating in D_2SO_4 and (3) etching by aqua regia are all effective ways to make a Pd cathode produce excess heat in subsequent closed-electrolysis of D_2O. The author once believed that these activations are valid for every Pd sample every time. However, after checking our past data for Pd plates, I found that all Pd samples showed the similar behavior as the Pd-B rod here, i.e., every Pd plate can only be activated a couple of times as listed in Tables 3 to 5. Tables 3 and 4 show Pd plates of #1 and #32, respectively, for pre-electrolysis activation and subsequent runs of calorimetry in electrolysis. It is found that Pd#1 produced the maximum excess power after the first two activations and Pd#32 produced the maximum excess power after the third activation. For activation of heating in D_2SO_4, Pd#16 produced the maximum excess power after the fourth activation as listed in Table 5. For activation of etching by aqua regia, only Pd#8 showed the maximum excess power after the first activation, as listed in Table 2 in Ref. [11] and no other sample was studied systematically due to etching process being hard to control.

On the other hand, Miles and Imam discussed another possibility, i.e., a cracked sample cannot produce excess heat [7]. As shown in Fig. 1(b), there are more than a dozen axial cracks of 0.15 mm width on the cylinder surface of

Table 3. Effects of cathode activation on excess power production for Pd#1 in D_2O closed electrolysis in Ref. [9].

#	$T_{activ,max}$/°C	R	$P_{ex,max}$/mW	I/A	t/h	date range
1	110	8/15	120(16)	0.03 - 3	167	081221 - 090907
2	97	4/4	115(24)	3 - 4	30	090908 - 090812
3	98	3/8	51(24)	0.3 - 3	71	090815 - 090906
4	108	0/1	17(22)	3	8	090916
5	145	0/2	31(22)	3	19	090918 - 090919
6	127	0/1	20(15)	3	7	090922
7	114	0/12	34(24)	0.1 - 3	99	090924 - 110523

Note: # is the ordinal number of cathode activation by open-electrolysis while DC power is set as 4 A and 18 V for 5 to 7.5 h. $P_{ex,max}$ is the maximum value of excess power under stable state ($P_{ex,max}$ listed in Table 3 of Ref. [9] was only instantaneous value, which was not stable and reliable after checking). Other symbols are the same as that in Table 1.

Table 4. Effects of cathode activation on excess power production for Pd#32 in D_2O closed electrolysis in Ref. [11].

#	$T_{activ,max}$/°C	R	$P_{ex,max}$/mW	I/A	t/h	date range
1	181	0/2	39(18)	4	27	150107 - 150110
2	196	0/1	40(16)	4	15	150112
3	213	1/1	100(32)	4.2	15	150116
4	188	1/2	30(15)	3 - 4.5	24	150121 - 150309
5	171	0/4	53(23)	3.5 - 4	48	150311 - 150326

Note: # is the ordinal number of cathode activation by open-electrolysis while DC power is set as 4 A and 18 V for 2 to 3.5 h. Other symbols are the same as that in Table 3.

Table 5. Effects of cathode activation on excess power production for Pd#16 in D_2O closed electrolysis in Ref. [11].

#	$T_{activ,max}$/°C	R	$P_{ex,max}$/mW	I/A	t/h	date range
1	235	1/1	61(24)	3.3	12	131231
2	242	0/1	-12(24)	3.3	8	140102
3	244	1/1	65(24)	3.3	12	140104
4	244	2/2	117(16)	3 - 3.3	36	140107 - 140110
5	241	1/2	29(16)	3 - 3.3	24	140122 - 140123

Note: # is the ordinal number of cathode activation by heating in D_2SO_4 for 1.5 to 2 h. Other symbols are the same as that in Table 3.

the Pd-B rod after 2,147 h of electrolysis. However, cracks with a width of 0.03 mm was observed as early as Mar. 18, 2021 (prior to Exp. #210318 shown in Fig. 9(a)), the cathode had been electrolyzed for 480 h and experienced one activation procedure before that day. Although the Pd-B rod did not produce pronounced excess heat at that time, it become activated after second activation on Feb. 20, 2022, as shown in Fig. 7. We are sure that the cracking on the Pd-B rod continuously grew during deuteriding-dedeuteriding in experiments due to radial plastic stresses developed in $\alpha \leftrightarrow \beta$ phase transition. Therefore, we cannot be sure that the cracking inhibits the excess heat, at least for this sample.

After 2,147 h of intermittent electrolysis, the Pd-B rod become thin at both ends and thick in the middle, as shown in the right of Fig. 1(b). Its average diameter of 12 points is 4.848 mm, therefore the total volume is 352.6 mm^3, which is only 2.4 mm^3 or 0.7% greater than the original volume of 350.2 mm^3. Storms studied the relationship between excess volume induced by deuteriding and dedeuteriding cycles and production of excess heat of Pd cathodes [14]–[16], and found that the excess volume of less than 1% of a sample does not increase even after repeated deuteriding-dedeuteriding, while the excess volume of greater than 1% of a sample increases with repeated deuteriding-dedeuteriding. The excess volume here is only 0.7%, which is less than 1%. Storms also found that excess volume no more than 2% is important for production of excess heat [15]. This means that the Pd-B rod here is a good

sample and B additive can suppress void production and expansion during deuteriding-dedeuteriding. One possible reason is that the concentration and volume changes of D during the $\alpha \leftrightarrow \beta$ phase transition in Pd-B are smaller than that in Pd [17], [18], resulting in a reduction in the plastic stress, so the void production is also less than that of pure palladium.

This cathode contains 0.25wt.% of boron (corresponding to $PdB_{0.025}$) and the actual boron content measured by glow-discharge mass spectroscopy (GDMS) is 0.18wt.% (corresponding to $PdB_{0.018}$) [19]. However, the original density of this rod according to the mass and volume in Section 1 is 11.758 g/cm^3, which is closed to that of $PdB_{0.05}$ and is smaller than that of $PdB_{0.025}$ or $PdB_{0.018}$ [20]. Although Pd-0.5wt.%B rods were manufactured at the same time and have the same dimensions as that of Pd-0.25wt.%B, M. A. Imam confirmed that the component of this rod is the latter. The reason of this inconsistency is unknown now. On the other hand, the volume expansion of this rod after repeated deuteriding and dedeuteriding cycles is different from the result of Pd containing 500 ppm boron in Ref. [16], where the presence of B leads to an increase in excess volume. One obvious reason is that the B content here is at least 36 times higher than in Storms [16].

This sample contains 10.3 mg of B and has a mass loss of 2.1 mg after long-duration electrolysis. Because it has been subjected to high temperature (218°C) electrolysis in D_2SO_4 in the first activation experiment as discussed above, we could not determine whether the mass loss was mainly due to the loss of B or the corrosion of Pd by sulfuric acid, because the electrode could not be weighed after it was spot-welded onto its Pt lead.

5. Conclusions

We reached four conclusions: First, The Pd-B cathode provided by Miles does produce excess heat. Second, Pre-electrolysis under high current and high temperature is an effective method to activate this cathode to produce excess heat during subsequent electrolysis. Third, the activation method is only effective the first few times it is applied. After that, applying it more times is disadvantageous. This experience applies not only to this Pd-B rod, but also to all samples of Pd plates studied in our lab. Finally, this sample expanded very little after repeated absorption and desorption of deuterium, meeting Storms' requirements for good Pd samples.

Although the detailed reason of present discovery is unclear now, it is a good start to improve the reproducibility and increase the magnitude of excess heat in Pd/D_2O electrolytic systems in the future.

Acknowledgments

The author thanks Profs. Melvin H. Miles and M. Ashraf Imam for providing the sample and helpful discussions. This work was supported by NSFC (22373106, 21153003, 20973185) and 973 program of MOST in China (2009CB226113).

References

[1] M. Fleischmann, S. Pons and M. Hawkins, Electrochemically induced nuclear fusion of deuterium. *J. Electroanal. Chem.* **261** (1989) 301–308. Erratum in **263** (1989) 187–188.

[2] M. Fleischmann, S. Pons, M.W. Anderson, L.J. Li and M. Hawkins, Calorimetry of the palladium-deuterium-heavy water system. *J. Electroanal. Chem.* **287** (1990) 293–348.

[3] M.C.H McKubre, S. Crouch-Baker, R.C. Rocha-Filho, S.I. Smedley, F.L. Tanzella, T.O. Passell and J. Santucci, Isothermal flow calorimetric investigations of the D/Pd and H/Pd systems, *J. Electroanal. Chem.* **368** (1994) 55–66.

[4] E. Storms, Use of a very sensitive Seebeck calorimeter to study the Pons–Fleischmann and Letts effects. *Proc. 10th Int. Conf. Cold Fusion*, P.L. Hagelstein and S.R. Chubb (Eds.), World Scientific, New York, 2006, pp. 183–197.

[5] M.H. Miles, R.A. Hollins, B.F. Bush, J.J. Lagowski and R.E. Miles, Correlation of excess power and helium production during D_2O and H_2O electrolysis using palladium cathodes. *J. Electroanal. Chem.* **346** (1993) 99–117.

[6] M.H. Miles, The Fleischmann–Pons calorimetric methods, equations and new applications. *J. Condensed Matter Nucl. Sci.* **24** (2017) 1–14.
[7] M.H. Miles and M.A. Imam, Excess power measurements for palladium–boron cathodes. *J. Condensed Matter Nucl. Sci.* **29** (2019) 12–20
[8] M.H. Miles, The Thermoneutral potential in electrochemical calorimetry for the Pd/D_2O System. *J. Condensed Matter Nucl. Sci.* **33** (2020) 74–80.
[9] W.-S. Zhang, Characteristics of excess heat in Pd|D_2O+D_2SO_4 electrolytic cells measured by Seebeck envelope calorimetry. *Proc. 15th Int. Conf. Condensed Matter Nuclear Science*, Roma, Italy, Oct. 5–9, 2009, pp. 27–32.
[10] W.-S. Zhang, Construction, calibration and testing of a decimeter-size heat-flow calorimeter. *Thermochim. Acta* **499** (2010) 128–132.
[11] J. Gao, W.-S. Zhang, J.-J. Zhang, Effects of D/Pd Ratio and cathode pretreatments on excess heat in closed Pd|D_2O + D_2SO_4 electrolytic cells. *J. Condensed Matter Nucl. Sci.* **24** (2017) 42–59.
[12] H. Zhao, W.-S. Zhang, W.-Y. Xiao, Excess heat in a Pd(Pt)-D_2O+LiOD reflux open-electrolytic cell, Presented at ICCF-23, Xiamen, China, June 7 to 9, 2021. See: http://lenr-canr.org/acrobat/ZhaoHexcessheat.pdf.
[13] W.-S. Zhang, A device and method for thermal power measurement. China Patent 201810191597.0.
[14] E. Storms, and C. Talcott-Storms, The effect of hydriding on the physical structure of palladium and on the release of contained tritium. *Fusion Technol.* **20** (1991) 246–257.
[15] E. Storms, How to produce the Pons-Fleischmann effect. *Fusion Technol.* **29** (1996) 261–268.
[16] E. Storms, Some thoughts on the nature of the nuclear-active regions in palladium. *The Sixth Int. Conf. on Cold Fusion, Progress in New Hydrogen Energy*, Hokkaido, Japan, Oct. 13–18, 1996. Vol. 1, pp. 105–112.
[17] R. Burch and F.A. Lewis, Absorption of Hydrogen by Palladium + Boron and Palladium + Silver + Boron Alloys. *Trans. Faraday Soc.* **66** (1970) 727–735.
[18] Y. Sakamoto, Y. Tanaka, K. Baba, T.B. Flanagan. Hydrogen Solubility in Palladium-Boron Alloys. *Z. Phys. Chem. N.F.* **158** (1988) S237–251.
[19] M.A. Imam, D.J. Nagel, M.H. Miles, Fabrication and characterization of palladium–boron alloys used in LENR experiments. *J. Condensed Matter Nucl. Sci.* **29** (2019) 1–11.
[20] M. Yoshihara, R.B. McLellan, Thermodynamics of the palladium-boron-hydrogen system. *Acta Metall. Mater*. **38** (1990) 655–661.